DOI: 10.1002/ejoc.201000436

A Combined Experimental and Theoretical Study of Anion–π Interactions in N^6- and N^9-Decyladenine Salts

Angel Garcia-Raso,[a] Francisca M. Albertí,*[a] Juan J. Fiol,[a] Yolanda Lagos,[a] Marta Torres,[a] Elies Molins,[b] Ignasi Mata,[b] Carolina Estarellas,[a] Antonio Frontera,*[a] David Quiñonero,[a] and Pere M. Deyà[a]

Keywords: Molecular recognition / Noncovalent interactions / Ab initio calculations / Pi interactions

We report the synthesis and X-ray characterization of N^9- and N^6-decyladenine hydrochloride salts. The latter exhibits interesting anion–π interactions, which are responsible for crystal packing. In contrast, the former does not present any anion–π interactions; the anion is stabilized by hydrogen-bonding interactions. Finally, a theoretical study of the different binding modes observed in the solid state is useful to explain the experimental findings.

Introduction

Noncovalent interactions are very important in modern chemistry, especially in the field of supramolecular chemistry, molecular recognition, and crystal engineering.[1] The latter deals with modeling, synthesis, evaluation, and utilization of crystalline solids having desired functions and fascinating architectures.[2–11] Certainly, the main complexity of this multidisciplinary branch is to rationalize synthesis to obtain a material with a given function. Any successful crystal engineering experiment tends to be very difficult to control, due to the delicate nature of a number of competing weak forces.[9,12] In this line, crystal structure prediction is a formidable exercise, which is very far from being fully resolved. The key to crystal structure prediction is precise understanding and complete control over the interplay of weak interactions responsible for crystal packing, when a number of them are operating simultaneously.[13–15]

Various weak interactions, such as hydrogen-bonding,[8,16–20] π–π stacking,[21–24] cation–π,[25] and CH–π[26,27] contacts are very common and well accepted among supramolecular chemists. For around eight years, a new type of supramolecular interaction, namely, the anion–π interaction,[28] has been increasingly reported in the literature, notwithstanding the preliminary improbability of considering repulsive interactions among the aromatic clouds and electron-rich molecules.[29–35] The design of highly selective anion receptors and channels represent important advances in this nascent field of supramolecular chemistry. Matile et al.[36] have also published remarkable synthetic ion channels based on anion–π interactions. The closely related lone pair (lp)–π interactions have been recently reviewed by Gamez et al.,[37] designating the lp–π contacts as a new supramolecular bond and rigorous analysis of the Cambridge Structure Database revealed that such contacts are not unusual in organic compounds, but have been overlooked in the past. Egli and co-workers studied the importance of lp–π interactions in biomacromolecules (Z-DNA and RNA[38]). Indeed, lp–π interactions have been found to be of great importance for the stabilization of biological macromolecules, as well as for the binding of inhibitors in the binding pocket of biochemical receptors.[39]

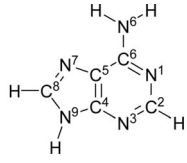

We have recently reported that the combination of a nucleobase (uracil) with a long aliphatic chain leads to a very interesting solid-state architecture that resembles a lipid bilayer.[40] The hydrogen-bond donor/acceptor capability of the nucleobase is responsible of the formation of a 2D hydrogen-bonding network that nicely stacks with another 2D layer through π–π interactions. Hydrophobic interactions between the aliphatic chains are responsible for the final architecture. Therefore, the intelligent combination of three weak noncovalent interactions guides to a fascinating structure. In addition, we have also demonstrated that the simple substitution of a hydrogen atom of the uracil ring by fluorine drastically changes the architecture. The effect of increasing the π acidity of the uracil ring by attaching one electron-withdrawing substituent triggers a change in the π–

[a] Department of Chemistry, Universitat de les Illes Balears, Crta. de Valldemossa km 7.5, 07122 Palma de Mallorca, Spain
Fax: +34-971-173426
E-mail: toni.frontera@uib.es
[b] Institut de Ciència de Materials de Barcelona (CSIC), Campus de la UAB, 08193 Cerdanyola, Barcelona, Spain

Supporting information for this article is available on the WWW under http://dx.doi.org/10.1002/ejoc.201000436.

π interaction, which is replaced by a lp–π interaction. Because the geometrical requirements of the π–π and lp–π interactions are very different, the effect on the crystal packing is very important. In this manuscript, by taking advantage of this previous knowledge, we have designed and synthesized two new compounds that are derivatives of adenine. We have decorated adenine with a long alkyl chain (C_{10}) to have a predefined ordering in the crystal due to hydrophobic effects. In addition, we have obtained the chlorohydrate salts to study whether anion–π interactions are formed and how they influence the final structure. We have previously demonstrated that protonated adenines and pyrimidines are well suited for establishing strong anion–π interactions with a variety of anions, including BF_4^-, NO_3^-, Cl^-, $ZnCl_4^{2-}$, and so on.[41] We have synthesized N^9-decyladenine and N^6-decyladenine hydrochloride salts, and we have obtained suitable crystals to be resolved for X-ray diffraction. Interestingly, in one structure relevant anion–π interactions are present and in the other the anion is stabilized only by hydrogen-bonding interactions. These noncovalent interactions are responsible for the differences in the crystal packing. We also report a high level ab initio study of the anion-binding properties of protonated N^9-decyladenine and N^6-decyladenine through hydrogen-bonding and anion–π interactions by using molecular interaction potential with polarization (MIPp)[42] calculations. The MIPp is a convenient tool for predicting binding properties. It has been successfully used for rationalizing molecular interactions such us hydrogen-bonding and ion–π interactions and for predicting molecular reactivity.[43] In particular, it has been found useful to predict the binding energy of a variety of π acidic rings, such as hexafluorobenzene,[28a] *s*-triazine,[43f] *s*-tetrazine,[43g] tricyanobenzene,[43h] isocyanuric acid,[28e] and so on.[43i] The MIPp partition scheme is an improved generalization of the molecular electrostatic potential (MEP), where three terms contribute to the interaction energy: (i) an electrostatic term identical to MEP,[44] (ii) a classical dispersion-repulsion term,[45] and (iii) a polarization term derived from perturbational theory.[46] We have found good agreement between the theoretical calculations and the solid-state structures. To analyze the intermolecular interactions, atoms-in-molecules (AIM) theory was employed.[47] AIM is based upon those critical points where the gradient of the density, $\nabla\rho$, vanishes. Such points are classified by the curvature of the electron density; for example, a bond critical point has one positive curvature (in the internuclear direction) and two negative ones (perpendicular to the bond). Two bonded atoms are then connected with a bond path through the bond critical point. The properties evaluated at such bond critical points characterize the bonding interactions. They have been widely used to study a great variety of molecular interactions.[47–49]

Results and Discussion

Synthesis of the Compounds

We have synthesized compounds **3** and **6** by using the following procedure, as shown in Scheme 1. Compound **2**[50] is easily prepared, in good yield (70%), from 6-chloropurine and decylamine under refluxing conditions in *n*BuOH/Et_3N. On the other hand, compound **5**[51] is obtained by reaction of adenine with sodium hydride in anhydrous DMF and subsequent addition of bromodecane. Dissolution of these compounds in EtOH/HCl 2 M yields the corresponding salts, **3** and **6**, respectively.

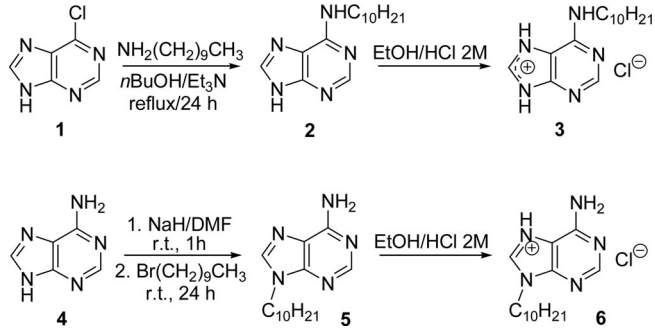

Scheme 1. Synthetic route to **3** and **6**.

Crystal Structure Description of 3 and 6

Compound **3** and **6** crystallize in the triclinic and monoclinic crystal system, respectively. The ORTEP diagrams of both compounds are shown in Figure 1. Selected bond lengths, angles, and supramolecular interactions are listed in Table 1, and crystallographic data collection and refinement parameters are listed in Table 2.

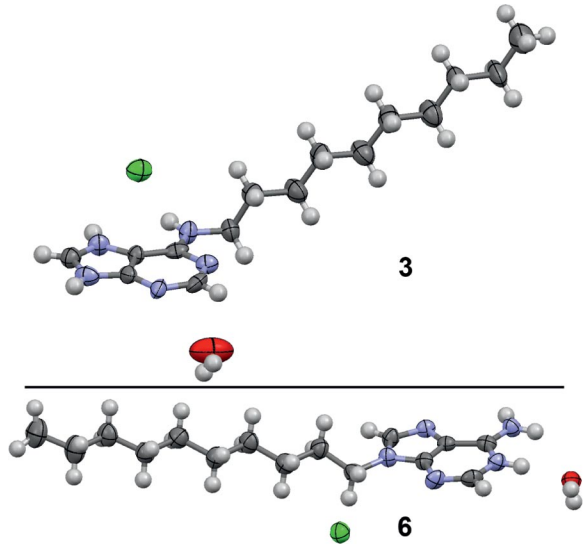

Figure 1. ORTEP diagrams of **3** (top) and **6** (bottom). Thermal ellipsoids are drawn at the 50% probability level.

In both solid-state structures, aliphatic chains form lipid-like layers alternated with layers of adenines, counterions, and solvent molecules. In these last layers, the compounds form planar dimers with both aliphatic chains oriented in opposite directions (Figure 2).

Table 1. Selected bond lengths [Å], angles [°], and supramolecular interactions in **3** and **6**.

Compound **3**[a]			
C(2)–N(3)	1.352(7)	C(5)–C(6)	1.401(8)
C(2)–N(1)	1.331(7)	C(6)–N(6)	1.340(7)
C(4)–N(9)	1.354(8)	C(6)–N(1)	1.368(8)
C(4)–C(5)	1.376(8)	C(8)–N(7)	1.328(7)
C(4)–N(3)	1.356(8)	C(8)–N(9)	1.321(7)
C(5)–N(7)	1.356(8)	C(10)–N(6)	1.452(7)
C(2)–N(1)–C(6)	118.5(6)	C(6)–N(6)–C(10)	124.3(6)
C(2)–N(3)–C(4)	115.7(6)	N(1)–C(6)–N(6)	116.5(7)
N(7)–C(8)–N(9)	112.7(6)		
D–H···A	*d*(H···A)	*d*(D···A)	∠(DHA)
N(6)–H(6)···Cl(1)#1	2.36	3.213(6)	170.2
N(7)–H(7)···Cl(1)#1	2.32(3)	3.105(5)	152(5)
N(9)–H(9)···N(3)#2	2.01	2.863(7)	169.2
Compound **6**[a]			
C(2)–N(3)	1.302(8)	C(5)–C(6)	1.425(8)
C(2)–N(1)	1.342(8)	C(6)–N(6)	1.300(8)
C(4)–N(9)	1.358(7)	C(6)–N(1)	1.361(8)
C(4)–C(5)	1.359(8)	C(8)–N(7)	1.317(7)
C(4)–N(3)	1.383(8)	C(8)–N(9)	1.366(8)
C(5)–N(7)	1.376(7)	C(10)–N(9)	1.471(7)
C(2)–N(1)–C(6)	123.9(5)	C(4)–N(9)–C(10)	126.3(5)
C(2)–N(3)–C(4)	110.3(6)	C(8)–N(9)–C(10)	128.3(5)
N(7)–C(8)–N(9)	114.0(5)		
D–H···A	*d*(H···A)	*d*(D···A)	∠(DHA)
N(1)–H(1)···O(1)	1.89(2)	2.784(6)	173(6)
N(6)–H(6A)···Cl(1)#1	2.43(4)	3.172(5)	147(5)
N(6)–H(6B)···N(7)#2	2.04(2)	2.892(8)	172(6)

[a] Symmetry transformations used to generate equivalent atoms in **3**: #1: $x-1, y, z$; #2: $-x+2, -y+1, -z+1$; in **6**: #1: $-x, -y+1, -z+1$; #2 $-x, -y, -z+1$.

Table 2. Crystallographic data for compounds **3** and **6**.

Compound	**3**	**6**
Empirical formula	$C_{15}H_{28}ClN_5O$	$C_{15}H_{27}ClN_5O_{0.5}$
Formula mass	329.87	320.87
Crystal system	triclinic	monoclinic
Space group	$P\bar{1}$(No. 2)	$C12/c1$ (No. 15)
Unit cell dimensions		
a [Å]	5.352(4)	39.859(10)
b [Å]	7.629(6)	4.961(3)
c [Å]	22.923(13)	18.572(9)
α [°]	93.34(4)	90
β [°]	95.60(4)	106.85(3)
γ [°]	98.23(3)	90
V [Å^3]	919.4(11)	3515(3)
Z	2	8
Density (calcd.) [Mg m^{-3}]	1.192	1.213
Absorption coefficient μ [mm^{-1}]	0.217	0.223
F(000)	356	1384
θ range for data collection [°]	1.79 to 24.97	1.07 to 25.99
Index ranges	$-6 \le h \le 6$	$-48 \le h \le 46$
	$-9 \le k \le 9$	$0 \le k \le 6$
	$0 \le l \le 27$	$0 \le l \le 22$
Reflections collected	3239	3435
Data/restraints/parameters	3239/5/209	3435/8/214
R_1 [$I>2\sigma(I)$]	0.1007	0.0974
wR_2 [$I>2\sigma(I)$]	0.1810	0.2541
R_1 (all data)	0.2176	0.2023
wR_2 (all data)	0.2151	0.2889
Goodness of fit on F^2	0.961	0.985
Largest diff. peak, hole [e Å^{-3}]	0.276, –0.303	0.363, –0.444

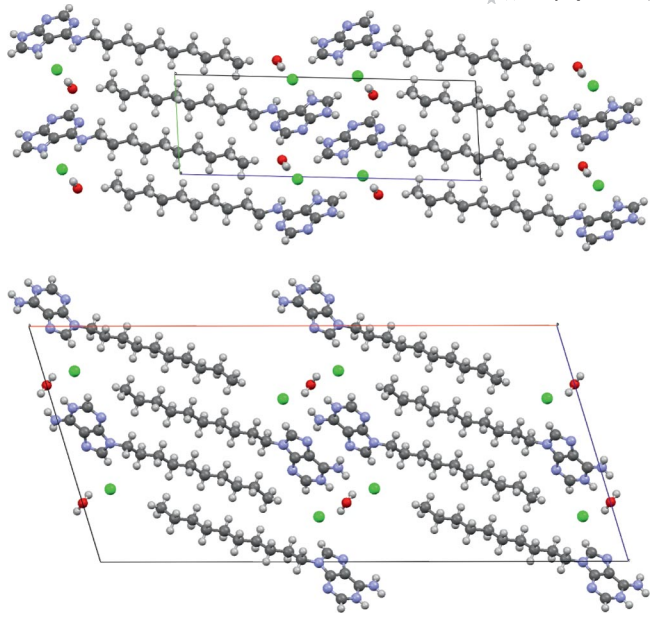

Figure 2. Crystal packing of **3** along (010) (top) and **6** along (001) (bottom).

The dimers are formed by double N–H···N donor/acceptor hydrogen bonds, forming $R^2_2(8)$ and $R^2_2(10)$ motifs in **3** and **6**, respectively. Those dimers are shown in Figure 3 together with the hydrogen-bonding interactions established in the molecular plane. Both motifs are frequent in adenine molecules and can be present in the same crystal structure for adeninium salts.[52] In this case, $R^2_2(8)$ is forbidden in **6** because of the substituent at N(9), whereas

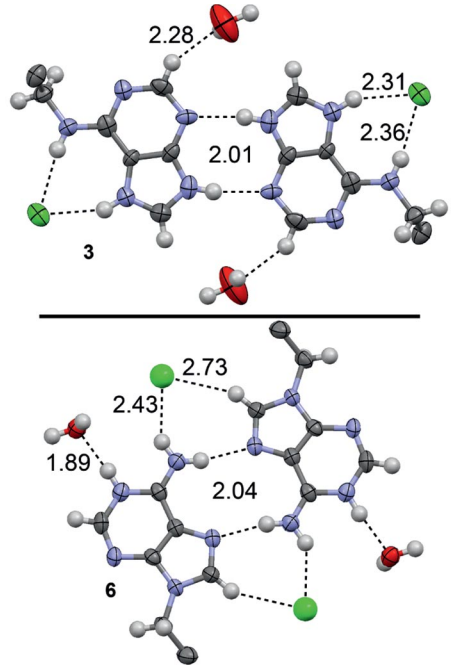

Figure 3. ORTEP drawing of the dimers of **3** and **6**. Thermal ellipsoids are drawn at the 50% probability level. Distances are given in Å. Long chains are omitted for clarity.

$R^2_2(10)$ seems to be unfavorable in **3** because of the substituent at N(6).

Chloride counterions are situated close to the molecular plane, acting as acceptors in hydrogen bonds with the N atoms. In both cases, the protonation sites are unambiguously fixed by the hydrogen-bond configuration, indicating that the N atom closer to the substitution site [N(1) in **3** and N(3) in **6**] is not protonated and is not involved in any intermolecular interaction. This atom seems to be under the influence of the hydrophobic part of the molecule, hence inaccessible to water or counterions.

In **3**, protonation takes place at N(7), which is somewhat unusual,[53] as the common protonation site in adenine derivatives that are N(6)-substituted is N(3) for either metallated complexes[54] or free ligands.[41c] This has important consequences in the H-bonding, as it allows the formation of the $R^2_2(8)$ motif while creating an electrophilic region around N(6) and N(7) where the chloride anion can be accommodated. Dimers form columns along (010) with their elements displaced and connected by O–H···Cl bonds involving a water molecule (Figure 4). There are additional C–H···O and C–H···Cl interactions along the adenine planes that group the dimers into tapes along (210) (Figure 5). This packing of adenines, chlorides, and water molecules is similar to that previously reported in other adenine salt.[55]

In **6**, the counterions bridge both molecules in the dimer, leaving the N(1) site available for interaction with a water molecule that adopts the same coordination as in the adeninium chloride.[56] The water molecule, which is situated in a crystallographic symmetry position, is acceptor in two N–H···O and donor in two O–H···Cl bonds (Figure 5). This hydrogen bonding scheme favors an almost perpendicular arrangement of the dimers at both sides of the water molecule (angle between adenine planes is 85.3°). As in **3**, columns of displaced dimers are formed, in this case along (001) (Figures 4 and 5), with the difference that, whereas in **3** molecules in all columns are parallel, in **6** molecules in contiguous columns are almost perpendicular.

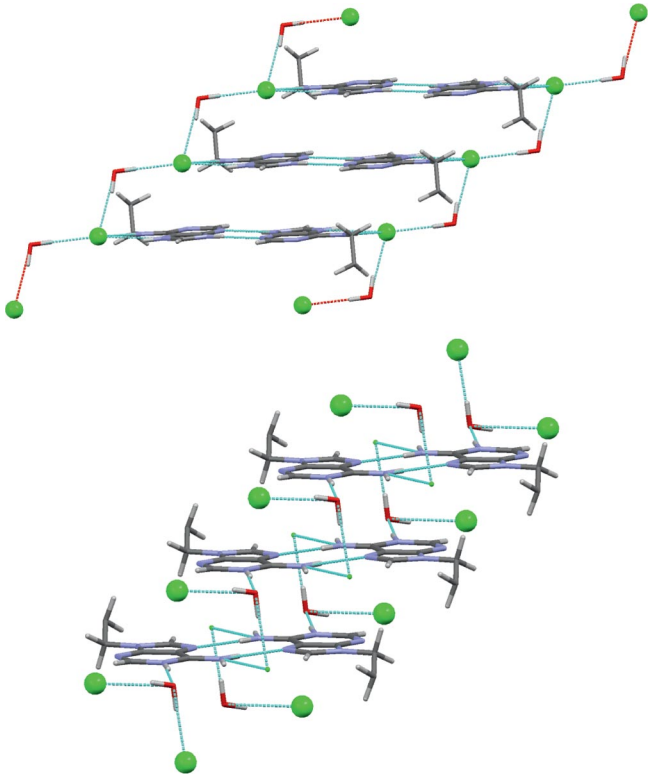

Figure 4. Columns of adenine dimers in **3** (top) and **6** (bottom). Long chains are omitted for clarity; chloride anions are represented by green spheres.

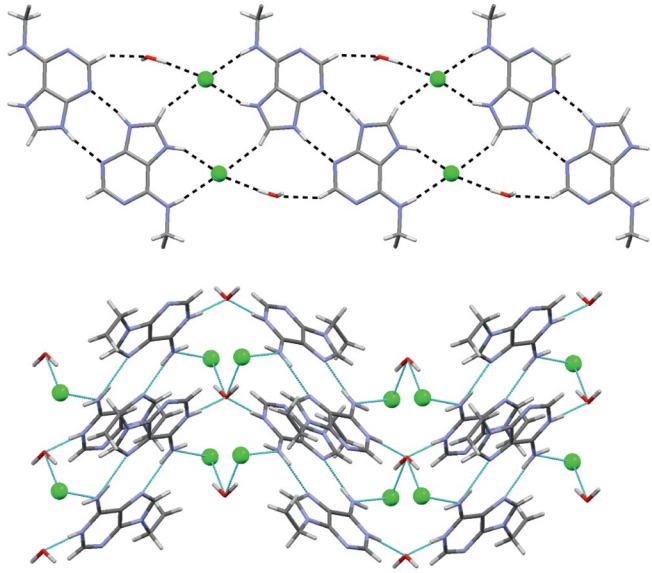

Figure 5. Interaction between dimers in contiguous columns: 1D tapes in **3** (top) and corrugated pattern in **6** (down). Long chains are omitted for clarity; chloride anions are represented by green spheres.

As stated in the introduction, one of the objectives of this work is to study the presence and influence of anion–π interactions in the solid-state structures of these compounds. From the ORTEP representation of the structures it can be easily appreciated that the chloride anion in **3** forms an anion–π interaction with the adenine moiety. In contrast, such interaction is not observed in compound **6**. A closer examination of the X-ray structure reveals that an anion–π/π–π/π–anion assembly is formed (see Figure 6). Similar findings of double anion–π interactions in condensed heterocycles have been described previously.[35,41c]

Supramolecular associations of types lp–π/π–π/π–lp and lp–π/π–π/π–anion have been previously reported in the solid-state structure of some transition and non-transition-metal–organic hybrid complexes. The potentiality of such newly discovered supramolecular forces in organizing and stabilizing molecular components in crystals has been proposed.[57] In compound **3**, the combination of the ordering obtained by the hydrophobic interactions of the decyl chains and the variety of interactions of the hydrophilic part gives rise to a very interesting crystal architecture (Figure 4). This variety of interactions includes the hydrogen-bonding network of the adenine dimer and the anion–π/π–π/π–anion association.[58]

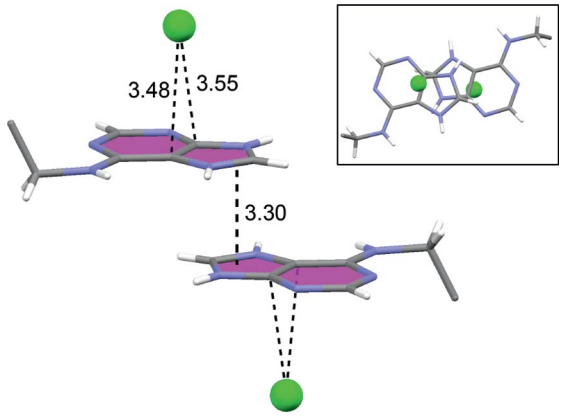

Figure 6. Detail of the anion–π/π–π/π–anion assembly in compound **3**. Distances are given in Å. Long chains are omitted for clarity; chloride anion is represented by a green sphere.

In compound **6**, anion–π interactions are not observed. In addition, adenine dimers do not form chains. The 2D hydrophilic part of the crystal is basically generated by hydrogen-bonding interactions (Figure 5, bottom). Apparently, π–π conventional stacking interactions between the adenine molecules are not present in the solid state. However, close examination reveals a pseudostacking binding mode that can be described as a double lp–π interaction, which is most likely enhanced by the fact that the rings are positively charged (Figure 7). The distance between the nitrogen atom belonging to the amino group of one adenine moiety and the ring centroid of the five-membered ring of the other adenine is 3.29 Å, which is shorter than the typical π–π stacking interaction. Interestingly, this value is very similar to the stacking interaction distance observed in compound **3** (see Figure 3) that is 3.31 Å. As a matter of fact, the π–π stacking interaction in **3** can be also described by a double lp–π interaction, because the nitrogen atom of the five-membered ring of one adenine is located approximately over the center of the five-membered ring of the other adenine.

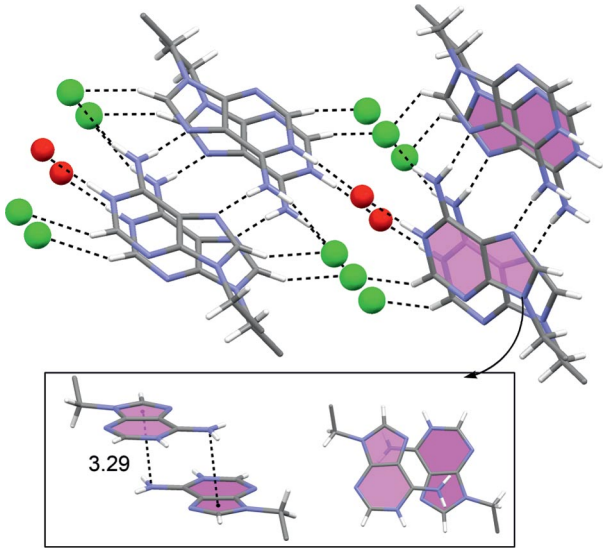

Figure 7. Hydrogen-bonding interactions in **6**. The double lp–π interaction is highlighted at the bottom. Distance from the nitrogen atom to the ring centroid is given in Å. The long chains and the hydrogen atoms of water are omitted for clarity. The chloride anions are represented by green spheres and oxygen atoms of water by red spheres.

It is interesting to compare the solid-state structure of the N^9-decyladenine hydrochloride salt with a neutral related molecule. In Figure 8, we show the structure of N^9-octyladenine, which was described previously by Salas et al.[59] It can be observed that the 3D architecture of the salt resembling a lipid bilayer is not observed in the neutral compound. This is basically due to the presence of CH–π interactions between the hydrogen atoms of the alkyl chain and the adenine aromatic rings. The CH–π interaction is very weak and it is replaced by stronger interactions like anion–π or lp–π contacts when the hydrochloride salt is formed.

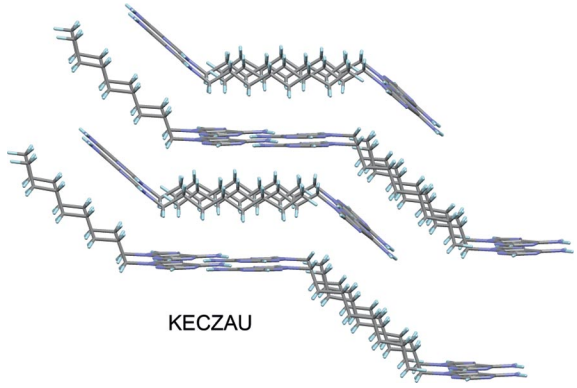

Figure 8. Crystal packing of KECZAU.

Theoretical Study

We have divided the theoretical study into three parts. First, we have compared the different hydrogen-bonding interaction modes of **3** and **6** to generate the adenine dimers observed in the solid state by computing the interaction energies. Second, we have computed 2D MIPp energy maps of compounds **3** and **6** to understand the different positions of the anion in the solid state. The MIPp calculations have been done with the MOPETE-98 program.[60] We have also compared the results obtained from the MIPp study with the energetic features of several anion–π complexes computed by ab initio calculations. Third, we have performed the AIM study of these anion–π complexes to characterize the interaction by obtaining the distribution of critical points that connect the anion with the aromatic ring.

For the first study, we have computed both dimers of adenine by using a theoretical model where the decyl chain has been substituted by a methyl group to reduce the computational cost. The binding energies, with the correction of the basis set superposition error (BSSE), and the optimized dimers are shown in Figure 9. We have used the MP2/6-31++G** level of theory in the Gaussian-03 package,[61] which is a good compromise between the accuracy of the

results and the computational cost. It can be observed that interaction energy (ΔE, BSSE corrected) of the dimer of **3** where the double N–H···N hydrogen bond forms a six-membered ring of heavy atoms is considerably more favorable than the one computed for the dimer of **6**, where the ring is formed by eight heavy atoms.

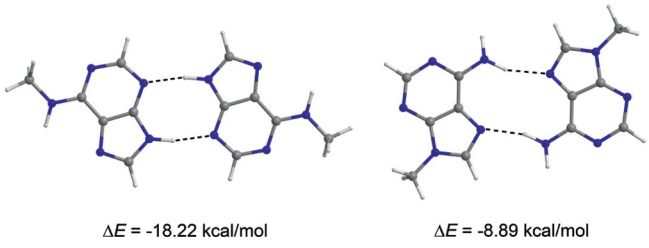

Figure 9. MP2/6-31++G** optimized structures of the dimers of **3** (left) and **6** (right). The interaction energies are also indicated.

For the second theoretical study, we computed the 2D MIPp maps at 3.5 Å above the molecular plane of several models of the crystal structures of **3** and **6** to study the spatial regions where the π interaction with Cl^- is more favorable. For **3**, we have used the dimer of adenine interacting with two chloride anions at the molecular plane to have a neutral system. The 2D MIPp map computed for the interaction of **3** with Cl^- is shown in Figure 10. It can be observed that there is a wide region where the lowest interaction potential isocontour line is located (red line). It can be appreciated that the location of the chloride anion in the crystal structure (see on-top representation of Figure 6) coincides with the lowest isocontour line. This result gives reliability to the MIPp method.

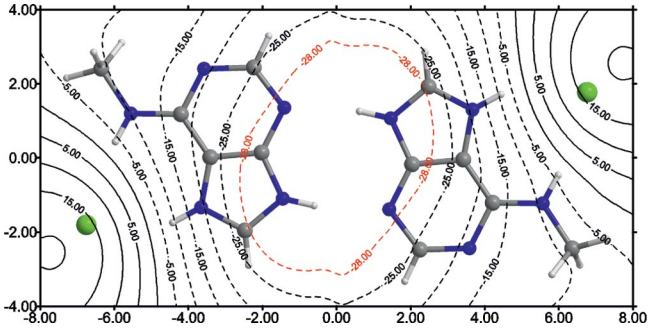

Figure 10. 2D MIPp(Cl^-) energy map of the dimer of **3** at a plane located at 3.5 Å above the molecular plane. Isocontour lines are drawn ever 5 kcal/mol apart from the lowest isocontour line (red line, –28 kcal/mol). Positive values of potential are represented by solid lines and negative values by dashed lines. Axes units are in Å.

The 2D MIPp map computed for the interaction of **6** with Cl^- is shown in Figure 11. As aforementioned, in the crystal structure of **6**, the protonated nitrogen atom of the adenine molecule does not interact directly with the counterion. Instead it forms a strong hydrogen-bonding interaction with a water molecule (Figure 3). We have used this complex (adenine–water) to compute the molecular interaction potential to study its π binding ability toward Cl^-. It can be observed in Figure 11 that the lowest isocontour line is found over one C–N bond of the six-membered ring of adenine. In the solid state (Figure 11, right) the position of the chloride nicely coincides with this region, over the isocontour line of –77 kcal/mol. A likely explanation for the differences in the π-binding ability of **3** and **6** is that in the latter the anion moves to the protonated nitrogen atom to counteract the excess amount of positive charge and to form a hydrogen bond with the hydrogen atoms of water. Consequently, an anion–π interaction is not established in this compound.

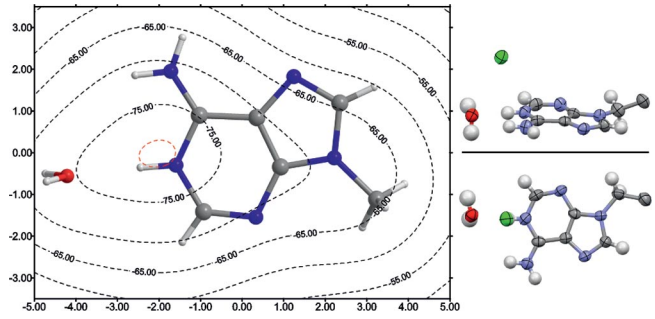

Figure 11. Left: 2D MIPp(Cl^-) energy map of the complex of **6** with water at a plane located at 3.5 Å above the molecular plane. Isocontour lines are drawn ever 5 kcal/mol apart from the lowest isocontour line (red line, –77 kcal/mol). Positive values of potential are represented by solid lines and negative values by dashed lines. Right: on-top (bottom) and perspective (top) views of a fragment of the crystal structure of **6** are represented. Long chains are omitted for clarity; axes units are in Å.

To further study the anion–π interactions observed in compound **3**, we computed the interaction energies of the anion–π complexes shown in Figure 12. Because the adenine molecules are protonated ($AdeH^+$), the interaction energy with chloride ion is expected to be very negative. Therefore, we used a neutral model, which is more realistic. We studied the energetic features of complexes **7** and **8** (Figure 12). In complex **7** the chloride ion interacts with the $AdeH^+$–Cl^- ionic pair as it is present in the solid state. The interaction energy (ΔE, BSSE corrected) is –15.6 kcal/mol, confirming the favorable anion–π binding ability of the ion pair, as it is observed in the X-ray structure. Interestingly, when a dimer of the $AdeH^+$–Cl^- ionic pair is used to compute the interaction energy, the value is more negative –25.15 kcal/mol (complex **8**), indicating that the presence of a second ionic pair forming the double N–H···N donor/acceptor hydrogen bond enhances the anion–π interaction. As a matter of fact, this interacting energy strongly agrees with the MIPp value computed in the 2D MIPp(Cl^-) energy map computed for **3** (Figure 10). This result also gives reliability to the energetic values obtained by the MIPp partition method. As aforementioned, the MIPp method decomposes the interaction energy in three terms, electrostatic E_e, polarization E_p, and dispersion–repulsion E_{vw}. The value of MIPp obtained from the 2D MIPp(Cl^-) energy map at the position where the Cl^- ion is located in the crystal structure (red contour in Figure 10, over the common

CC bond of adenine) is –28.06 kcal/mol. In this point the three contributions are E_e = –19.52 kcal/mol, E_p = –7.13 kcal/mol, and E_{vw} = –1.41 kcal/mol, indicating that the anion–π interaction in this system is basically dominated by electrostatic effects. The polarization term is not negligible and it also contributes to the overall stabilization of the system. In contrast, the van der Waals term is modest.

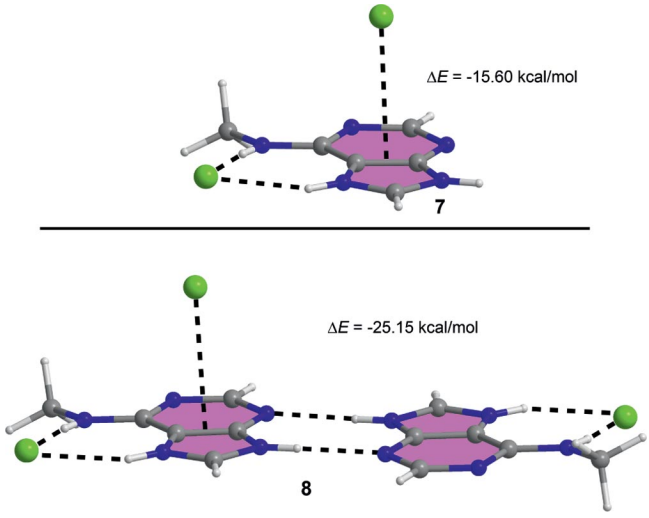

Figure 12. Anion–π complexes **7** (top) and **8** (bottom) and their corresponding binding energies (MP2/6-31++G**, BSSE corrected) computed considering that the $AdeH^+$–Cl^- (top) or the adenine dimer $(AdeH^+–Cl^-)_2$ (bottom) has been previously formed.

Finally, we performed AIM analysis of both anion–π complexes **7** and **8**. The distribution of critical points that characterize the noncovalent interactions is shown in Figure 13. In both complexes the anion–π interaction is characterized by the presence of one bond critical point (BCP, red sphere) that connects the anion with the aromatic ring and the Cl^-···H–N bifurcated hydrogen-bond interaction is characterized by the presence of two BCPs and one ring critical point (RCP, yellow sphere). Finally, the double N–H···N donor/acceptor hydrogen bond of complex **8** is characterized by the presence of two BCPs and one RCP. In all critical points the value of the Laplacian of the charge density (ρ) is positive, as is common in closed-shell interactions.[47] It has been demonstrated that the value of ρ at the BCP can be used as a measure of the strength of the interaction.[43d] It can be appreciated that the value of ρ at the BCP in complex **7** is smaller than in complex **8**. Therefore, from Bader's analysis it can be deduced that the strength of the anion–π interaction in complex **7** is larger than that in complex **8**, in agreement with the MP2/6-31++G** energetic results.

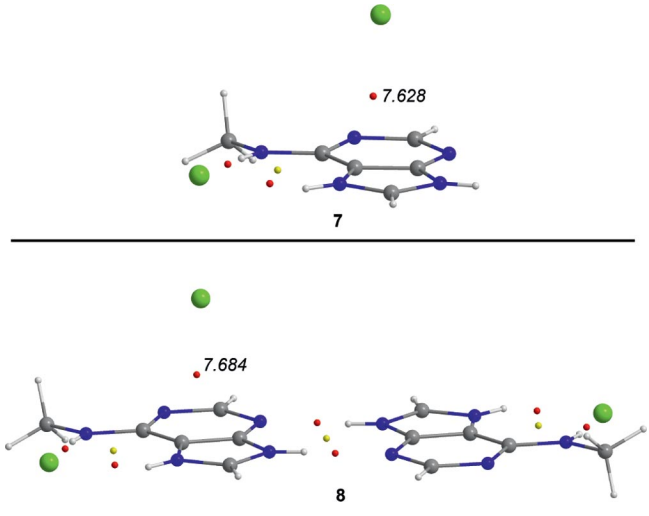

Figure 13. Distribution of critical points obtained for anion–π complexes **7** (top) and **8** (bottom). The values of the charge density ($10^2 \times \rho$, a.u.) are in italics. Bond and ring critical points are represented by small red and yellow spheres, respectively.

Conclusions

To conclude, we have synthesized and X-ray characterized two new compounds, N^9- and N^6-decyladenine hydrochloride salts, that illustrate the importance of anion–π, π–π, and hydrophobic interactions in supramolecular chemistry. The intelligent combination of long aliphatic chains and the versatility of nucleic bases to establish a variety of noncovalent interactions can be used to obtain fascinating architectures in the solid state. The 2D MIPp energy maps are in good agreement with the X-ray structures, as they are able to predict the spatial regions where the interaction of the anion with the ring is more favorable. Finally, crystal engineering comprises indepth understanding of weak intermolecular forces that govern crystal packing, thus potentially allowing rational design of solids with tailored physical and chemical properties. The results described above are certainly of importance in this regard and certainly help to gain knowledge in this emerging area of supramolecular chemistry.

Experimental Section

General Methods: Melting points were determined with a Gallenkamp instrument. Elemental analyses were carried out by using Carlo–Erba models 1106 and 1108 and Thermo Finningan Flash 1112 microanalyzers. Infrared spectra (KBr pellets) were recorded with a Bruker IFS 66. ^1H and ^{13}C NMR spectra were obtained with a Bruker AMX 300 spectrometer. Proton and carbon chemical shifts in dimethyl sulfoxide were referenced to [D_6]DMSO itself [^1H NMR: δ(DMSO) = 2.47 ppm; ^{13}C NMR: δ(DMSO) = 40.0 ppm]. All organic and inorganic (Sigma and Aldrich) reagents were used without further purification.

***N*^{6}-Decyladenine (*N*^{6}-AdeC$_{10}$; 2):** Easily prepared, in good yield (70%), from 6-chloropurine and decylamine under refluxing conditions in *n*BuOH/Et_3N. A complete spectroscopic (IR, NMR spectra) and analytical (elemental analysis, melting point) characterization is given in the Supporting Information

***N*^{6}-AdeC$_{10}$·HCl (3):** Obtained as a crystalline material by evaporation of the ligand (50 mg) dissolved in EtOH/HCl 2 M. Yield: 40 mg (70%). M.p. 192–194 °C. $C_{15}H_{27.5}ClN_5O_{0.75}$ (325.37): calcd. C

55.37, H 8.52, N 21.52; found C 55.15, H 8.59, N 21.63. IR: $\tilde{\nu}$ = 3534 (m), 3105 (m), 2915 (s), 2847 (s), 1661 (vs), 1614 (s), 1584 (m), 1514 (m), 1490 (m), 1464 (s), 1450 (s), 1431 (m), 1399 (s), 1370 (m), 1351 (s), 1286 (m), 1206 (s), 800 (m), 777 (s), 616 (s), 524 (m) cm^{-1}. ^1H NMR (300 MHz, [D_6]DMSO): δ = 9.70 (br. s, 1 H, N9-H), 8.55 (s, 1 H, 2-H), 8.49 (s, 1 H, 8-H), 1.60 (br. quint., 2 H, 11-H), 1.19 (br. m, 14 H, 12-H, 13-H, 14-H, 15-H, 16-H, 17-H, 18-H), 0.80 (br. t, 3 H, 19-H) ppm. ^{13}C NMR (300 MHz, [D_6]DMSO): δ = 151.5 (C-6), 147.5 (C-4), 147.0 (C-2), 143.8 (C-8), 112.6 (C-5), 41.7 (C-10), 31.8, 29.4, 29.2, 28.8, 26.8, 22.6 (C-11, C-12, C-13, C-14, C-15, C-16, C-17, C-18), 14.5 (C-19) ppm. Few crystals of composition $C_{30}H_{52}Cl_2N_{10}O$ were suitable for X-ray studies.

***N*^{9}-Decyladenine (*N*^{9}-AdeC$_{10}$; 5):** Obtained by reaction of adenine with sodium hydride in anhydrous DMF and subsequent addition of bromodecane. Complete spectroscopic (IR, NMR spectra) and analytical (elemental analysis, melting point) characterization is given in the Supporting Information

***N*^{9}-AdeC$_{10}$·HCl (6):** Obtained as a crystalline material by evaporation of the ligand (150 mg) dissolved in EtOH/HCl 2 M after several months. Yield: 85 mg (50%). M.p. 182–184 °C. $C_{15}H_{27}ClN_5O_{0.5}$ (320.86): calcd. C 56.15, H 8.48, N 21.83; found C 56.26, H 8.69, N 21.89. IR: $\tilde{\nu}$ = 3491 (m), 3373 (m), 2920 (s), 2852 (s), 1697 (m), 1669 (s), 1612 (m), 1602 (sh.), 1487 (m), 1456 (m), 1395 (m), 1374 (m), 1344 (m), 1216 (m), 774 (m), 619 (m) cm^{-1}. ^1H NMR (300 MHz, [D_6]DMSO): δ = 8.45 (s, 1 H, 2-H), 8.40 (s, 1 H, 8-H), 4.18 (t, $^3J_{H,H}$ = 7.2 Hz, 2 H, 10-H), 1.78 (br. m, 2 H, 11-H), 1.18 (br. m, 14 H, 12-H, 13-H, 14-H, 15-H, 16-H, 17-H, 17-H, 18-H), 0.82 (br. t, 3 H, 19-H) ppm. ^{13}C NMR (300 MHz, [D_6]DMSO): δ = 150.9 (C-6), 149.0 (C-2), 145.4 (C-4), 144.5 (C-8), 118.4 (C-5), 44.2 (C-10), 31.8, 29.8, 29.3, 29.1, 28.9 (C-11, C-12, C-13, C-14, C-15, C-16), 26.3 (C-17), 22.6 (C-18), 14.4 (C-19) ppm.

X-ray Crystallographic Studies: Suitable crystals of **3** and **6** were selected for X-ray single crystal diffraction experiments and mounted at the tips of glass fibers on an Enraf–Nonius CAD4 diffractometer producing graphite monochromated Mo-K_α radiation (λ = 0.71073 Å). After the random search of 19 (in **3**) and 25 reflections (in **6**), the indexation procedure gave rise to the cell parameters. Intensity data were collected in the ω-2θ scan mode and corrected for Lorenz and polarization effects. Absorption correction was performed by following the empirical DIFABS method.[62] The structural resolution procedure was made by using the WinGX package.[63] Solving for structure factor phases was performed with SHELXS86[64] for **3** and with SIR2004[65] for **6**, and the full-matrix refinement with SHELXL97.[66] Non-hydrogen atoms were refined anisotropically and all hydrogen atoms were introduced in calculated positions and refined riding on their parent atoms, except for water molecules and the protonation sites (located in the Fourier differences maps). A summary of refinement parameters can also be seen in Table 2. We repeatedly tried to obtain better quality crystals for compounds **3** and **6**, but our attempts were unsuccessful possibly due to the long aliphatic chain present in those compounds. CCDC-771374 (for **3**) and -771375 (for **6**) contain the supplementary crystallographic data for this paper. These data can be obtained free of charge from The Cambridge Crystallographic Data Centre via www.ccdc.cam.ac.uk/data_request/cif.

Supporting Information (see footnote on the first page of this article): IR, ^1H NMR, and ^{13}C NMR spectra and elemental analysis of synthesized compounds; Cartesian coordinates of optimized dimer of **3** and **6**.

Acknowledgments

We thank the "Dirección General de Investigación, Ciencia y Tecnología" (DGICYT) of Spain (projects CTQ2008-00841/BQU, CTQ2009-12520-C03-03, and CONSOLIDER CSD2007-00041) and the Generalitat de Catalunya (Grant No. 2009SGR-203) for financial support. We thank the "Centre de Supercomputació de Catalunya" (CESCA) for computational facilities. I.M. thanks the Institut de Ciència de Materials de Barcelona (CSIC) for a JAE-Doc fellowship financed by the European Social Fund. C.E. thanks the "Ministerio de Educación y Ciencia" (MEC) for an undergraduate fellowship. D.Q. thanks the Ministerio de Ciencia e Innovación (MICINN) for a "Ramón y Cajal" contract. F.M.A. thanks the "Conselleria d'Economia, Hisenda i Innovació del Govern de les Illes Balears" (Spain) and "Fons Social Europeu" (FSE) for a contract as an investigation support technician.

[1] E. A. Meyer, R. K. Castellano, F. Diederich, *Angew. Chem. Int. Ed.* **2003**, *42*, 1210–1250.
[2] G. R. Desiraju, *Crystal Engineering: The Design of Organic Solids*, Elsevier, Amsterdam, The Netherlands, **1989**.
[3] K. Biradha, *CrystEngComm* **2003**, *5*, 374–384.
[4] M. J. Zaworotko, *Chem. Commun.* **2001**, 1–9.
[5] K. T. Holman, A. M. Pivovar, J. A. Swift, M. D. Ward, *Acc. Chem. Res.* **2001**, *34*, 107–118.
[6] C. B. Aakeröy, A. M. Beatty, B. A. Helfrich, *Angew. Chem. Int. Ed.* **2001**, *40*, 3240–3242.
[7] C. B. Aakeröy, *Acta Crystallogr., Sect. B* **1997**, *53*, 569–586.
[8] G. R. Desiraju, *Acc. Chem. Res.* **2002**, *35*, 565–573.
[9] L. Brammer, *Chem. Soc. Rev.* **2004**, *33*, 476–489.
[10] D. Braga, L. Brammer, N. R. Champness, *CrystEngComm* **2005**, *7*, 1–19.
[11] a) D. Braga, G. R. Desiraju, J. S. Miller, A. G. Orpen, S. L. Price, *CrystEngComm* **2002**, *4*, 500–509; b) B. H. Hong, S. C. Bae, C.-W. Lee, S. Jeong, K. S. Kim, *Science* **2001**, *294*, 348–351; c) N. J. Singh, H. M. Lee, I.-C. Hwang, K. S. Kim, *Supramol. Chem.* **2007**, *19*, 321–332.
[12] a) A. D. Jana, S. C. Manna, G. M. Rosair, M. G. B. Drew, G. Mostafa, N. R. Chaudhuri, *Cryst. Growth Des.* **2007**, *7*, 1365–1372 and references cited therein; b) N. J. Singh, H. M. Lee, S. B. Suh, K. S. Kim, *Pure Appl. Chem.* **2007**, *79*, 1057–1075; c) J. Y. Lee, B. H. Hong, W. Y. Kim, S. K. Min, Y. Kim, M. V. Jouravlev, R. Bose, K. S. Kim, I.-C. Hwang, L. J. Kaufman, C. W. Wong, P. Kim, K. S. Kim, *Nature* **2009**, *460*, 498–501.
[13] S. Samai, K. Biradha, *CrystEngComm* **2009**, *11*, 482–492.
[14] T. S. Thakur, G. R. Desiraju, *Cryst. Growth Des.* **2008**, *8*, 4031–4044.
[15] S. L. Price, *Acc. Chem. Res.* **2009**, *42*, 117–126.
[16] G. A. Jeffrey, *An Introduction to Hydrogen Bonding*, Oxford University Press, Oxford, **1997**.
[17] G. R. Desiraju, T. Steiner, *The Weak Hydrogen Bond in Structural Chemistry and Biology*, Oxford University Press, Oxford, **1999**.
[18] G. R. Desiraju, *Nature* **2001**, *412*, 397–400.
[19] a) A. M. Beatty, *CrystEngComm* **2001**, *51*, 1–13; b) C. Pak, H. M. Lee, J. C. Kim, D. Kim, K. S. Kim, *Struct. Chem.* **2005**, *16*, 187–202; c) H. M. Lee, S. B. Suh, J. Y. Lee, P. Tarakeshwar, K. S. Kim, *J. Chem. Phys.* **2000**, *112*, 9759–9772; d) B. H. Hong, J. Y. Lee, C.-W. Lee, J. C. Kim, S. C. Bae, K. S. Kim, *J. Am. Chem. Soc.* **2001**, *123*, 10748–10749.
[20] T. Steiner, *Angew. Chem. Int. Ed.* **2002**, *41*, 48–76.
[21] a) C. A. Hunter, J. K. M. Sanders, *J. Am. Chem. Soc.* **1990**, *112*, 5525–5534; b) S. K. Burley, G. A. Petsko, *Science* **1985**, *229*, 23–28.
[22] a) K. S. Kim, P. Tarakeshwar, J. Y. Lee, *Chem. Rev.* **2000**, *100*, 4145–4185; b) E. C. Lee, D. Kim, P. Jurecka, P. Tarakeshwar, P. Hobza, K. S. Kim, *J. Phys. Chem. A* **2007**, *111*, 3446–3457; c)

N. J. Singh, S. K. Min, D. Y. Kim, K. S. Kim, *J. Chem. Theor. Comput.* **2009**, *5*, 515–529.
[23] C. J. Janiak, *J. Chem. Soc., Dalton Trans.* **2000**, 3885–3896.
[24] E. A. Meyer, R. K. Castellano, F. Diederich, *Angew. Chem. Int. Ed.* **2003**, *42*, 1210–1250.
[25] a) J. C. Ma, D. A. Dougherty, *Chem. Rev.* **1997**, *97*, 1303–1324; b) D. Kim, S. Hu, P. Tarakeshwar, K. S. Kim, J. M. Lisy, *J. Phys. Chem. A* **2003**, *107*, 1228–1238; c) K. S. Kim, J. Y. Lee, S. J. Lee, T.-K. Ha, D. H. Kim, *J. Am. Chem. Soc.* **1994**, *116*, 7399–7400.
[26] a) M. Nishio, M. Hirota, Y. Umezawa, *The C–H/π Interaction: Evidence, Nature and Consequences*, Wiley-VCH, New York, **1998**; b) M. Nishio, *CrystEngComm* **2004**, *6*, 130–158.
[27] a) S. K. Burley, G. A. Petsko, *Science* **1985**, *229*, 23–28; b) K. S. Kim, P. Tarakeshwar, J. Y. Lee, *J. Am. Chem. Soc.* **2001**, *123*, 3323–3331.
[28] a) D. Quiñonero, C. Garau, C. Rotger, A. Frontera, P. Ballester, A. Costa, P. M. Deyà, *Angew. Chem. Int. Ed.* **2002**, *41*, 3389–3392; b) I. Alkorta, I. Rozas, J. Elguero, *J. Am. Chem. Soc.* **2002**, *124*, 8593–8598; c) M. Mascal, A. Armstrong, M. Bartberger, *J. Am. Chem. Soc.* **2002**, *124*, 6274–6276; d) M. Mascal, *Angew. Chem. Int. Ed.* **2006**, *45*, 2890–2893; e) A. Frontera, F. Saczewski, M. Gdaniec, E. Dziemidowicz-Borys, A. Kurland, P. M. Deyà, D. Quiñonero, C. Garau, *Chem. Eur. J.* **2005**, *11*, 6560–6567.
[29] a) G. Gil-Ramirez, E. C. Escudero-Adan, J. Benet-Buchholz, P. Ballester, *Angew. Chem. Int. Ed.* **2008**, *47*, 4114–4118; b) T. J. Mooibroek, C. A. Black, P. Gamez, J. Reedijk, *Cryst. Growth Des.* **2008**, *8*, 1082–1093.
[30] a) D. Kim, P. Tarakeshwar, K. S. Kim, *J. Phys. Chem. A* **2004**, *108*, 1250–1258; b) D. Kim, E. C. Lee, K. S. Kim, P. Tarakeshwar, *J. Phys. Chem. A* **2007**, *111*, 7980–7986; c) D. Y. Kim, N. J. Singh, J. W. Lee, K. S. Kim, *J. Chem. Theor. Comput.* **2008**, *4*, 1162–1169; d) D. Y. Kim, N. J. Singh, K. S. Kim, *J. Chem. Theor. Comput.* **2008**, *4*, 1401–1407.
[31] P. Gamez, T. J. Mooibroek, S. J. Teat, J. Reedijk, *Acc. Chem. Res.* **2007**, *40*, 435–444.
[32] B. L. Schottel, H. T. Chifotides, K. R. Dunbar, *Chem. Soc. Rev.* **2008**, *37*, 68–83.
[33] B. P. Hay, V. S. Bryantsev, *Chem. Commun.* **2008**, 2417–2428.
[34] R. J. Götz, A. Robertazzi, I. Mutikainen, U. Turpeinen, P. Gamez, J. Reedijk, *Chem. Commun.* **2008**, 3384–3386 and references cited therein.
[35] a) I. A. Guralskiy, P. V. Solntev, H. Krautscheid, K. V. Domasevitch, *Chem. Commun.* **2006**, 4808–4810; b) K. V. Domasevitch, P. V. Solntev, I. A. Guralskiy, H. Krautscheid, E. B. Rusanov, A. N. Chernega, J. A. K. Howard, *Dalton Trans.* **2007**, 3893–3905.
[36] a) J. Mareda, S. Matile, *Chem. Eur. J.* **2008**, *15*, 28–37; b) V. Gorteau, G. Bollot, J. Mareda, A. Perez-Velasco, S. Matile, *J. Am. Chem. Soc.* **2006**, *128*, 14788–14789; c) V. Gorteau, G. Bollot, J. Mareda, S. Matile, *Org. Biomol. Chem.* **2007**, *5*, 3000–3012; d) V. Gorteau, M. D. Julliard, S. Matile, *J. Membr. Sci.* **2008**, *321*, 37–42; e) A. Perez-Velasco, V. Gorteau, S. Matile, *Angew. Chem.* **2008**, *120*, 935–939; f) R. E. Dawson, A. Hennig, D. P. Weimann, D. Emery1, V. Ravikumar, J. Montenegro, T. Takeuchil, S. Gabutti, M. Mayor, J. Mareda, C. A. Schalley, S. Matile, *Nature Chem.* **2010**, *2*, 533–538.
[37] T. J. Mooibroek, P. Gamez, J. Reedijk, *CrystEngComm* **2008**, *10*, 1501–1515.
[38] a) M. Egli, S. Sarkhel, *Acc. Chem. Res.* **2007**, *40*, 197–205; b) M. Egli, R. V. Gessner, *Proc. Natl. Acad. Sci. USA* **1995**, *92*, 180–184; c) S. Sarkhel, A. Rich, M. Egli, *J. Am. Chem. Soc.* **2003**, *125*, 8998–8999.
[39] J. C. Calabrese, D. B. Jordan, A. Boodhoo, S. Sariaslani, T. Vannelli, *Biochemistry* **2004**, *43*, 11403–11416.
[40] M. Barceló-Oliver, C. Estarellas, A. Garcia-Raso, A. Terrón, A. Frontera, D. Quiñonero, E. Molins, P. M. Deyà, *CrystEngComm* **2010**, *12*, 362–365.
[41] a) A. Garcia-Raso, F. M. Alberti, J. J. Fiol, A. Tasada, M. Barceló-Oliver, E. Molins, C. Estarellas, A. Frontera, D. Quiñonero, P. M. Deyà, *Cryst. Growth Des.* **2009**, *9*, 2363–2376; b) A. Garcia-Raso, F. M. Alberti, J. J. Fiol, A. Tasada, M. Barceló-Oliver, E. Molins, D. Escudero, A. Frontera, D. Quiñonero, P. M. Deyà, *Eur. J. Org. Chem.* **2007**, *35*, 5821–5825; c) A. Garcia-Raso, F. M. Alberti, J. J. Fiol, A. Tasada, M. Barceló-Oliver, E. Molins, D. Escudero, A. Frontera, D. Quiñonero, P. M. Deyà, *Inorg. Chem.* **2007**, *46*, 10724–10735.
[42] F. J. Luque, M. Orozco, *J. Comput. Chem.* **1998**, *19*, 866–881.
[43] a) B. Hernández, M. Orozco, F. J. Luque, *J. Comput-Aided Mol. Des.* **1997**, *11*, 153–171; b) F. J. Luque, M. Orozco, *J. Chem. Soc. Perkin Trans. 2* **1993**, 683–690; c) D. Quiñonero, A. Frontera, G. A. Suñer, J. Morey, A. Costa, P. Ballester, P. M. Deyà, *Chem. Phys. Lett.* **2000**, *326*, 247–254; d) D. Quiñonero, A. Frontera, C. Garau, P. Ballester, A. Costa, P. M. Deyà, *ChemPhysChem* **2006**, *7*, 2487–2491; e) C. Garau, D. Quiñonero, A. Frontera, P. Ballester, A. Costa, P. M. Deyà, *J. Phys. Chem. A* **2005**, *41*, 9341–9345; f) C. Garau, D. Quiñonero, A. Frontera, P. Ballester, A. Costa, P. M. Deyà, *Org. Lett.* **2003**, *5*, 2227–2229; g) C. Garau, D. Quiñonero, A. Frontera, P. Ballester, A. Costa, P. M. Deyà, *Chem. Phys. Lett.* **2003**, *370*, 7–13; h) C. Garau, A. Frontera, P. Ballester, D. Quiñonero, A. Costa, P. M. Deyà, *Eur. J. Org. Chem.* **2005**, 179–183; i) C. Garau, A. Frontera, D. Quiñonero, P. Ballester, A. Costa, P. M. Deyà, *Recueil Res. Develop. Chem. Phys.* **2004**, *5*, 227–255.
[44] E. Scrocco, J. Tomasi, *Top. Curr. Chem.* **1973**, *42*, 95–170.
[45] M. Orozco, F. J. Luque, *J. Comput. Chem.* **1993**, *14*, 587–602.
[46] M. M. Francl, *J. Phys. Chem.* **1985**, *89*, 428–433.
[47] R. F. W. Bader, *Chem. Rev.* **1991**, *91*, 893–928.
[48] R. F. W. Bader, *Atoms in Molecules – A Quantum Theory*, Oxford, University Press, Oxford, **1990**.
[49] a) S. J. Grabowski, A. Pfitzner, M. Zabel, A. T. Dubis, M. Palusiak, *J. Phys. Chem. B* **2004**, *108*, 1831–1837; b) A. Vila, R. A. Mosquera, *THEOCHEM* **2001**, *546*, 63–72; c) D. Chopra, T. S. Cameron, J. D. Ferrara, T. N. Guru Row, *J. Phys. Chem. A* **2006**, *110*, 10465–10477.
[50] a) G. B. Elion, E. Burgi, G. H. Hitchings, *J. Am. Chem. Soc.* **1952**, *74*, 411–414; b) M. Sutherland, B. E. Christensen, *J. Am. Chem. Soc.* **1957**, *79*, 2251–2252.
[51] S.-H. Lu, S. Selvi, J.-M. Fang, *J. Org. Chem.* **2007**, *72*, 117–122. Cited in this reference, but no experimental data was found.
[52] See, for example, B. E. Hingerty, J. R. Einstein, C. H. Wei, *Acta Crystallogr., Sect. B* **1981**, *37*, 140–147.
[53] See, for example: B. Lippert, *Coord. Chem. Rev.* **2000**, *200–202*, 487–516.
[54] See, for example: a) J. J. Fiol, A. Garcia-Raso, F. M. Albertí, A. Tasada, M. Barceló-Oliver, A. Terrón, M. J. Prieto, V. Moreno, E. Molins, *Polyhedron* **2008**, *27*, 2851–2858; b) T. P. Balasubramanian, P. T. Muthiah, Ananthasaravanan, S. K. Mazumdar, *J. Inorg. Biochem.* **1996**, *63*, 175–181.
[55] Y.-J. Cheng, Z.-M. Wang, C.-S. Liao, C.-H. Yan, *New J. Chem.* **2002**, *26*, 1360–1364.
[56] L. M. Cunane, M. R. Taylor, *Acta Crystallogr., Sect. B* **1993**, *49*, 524–530.
[57] I. Alkorta, F. Blanco, P. M. Deyà, J. Elguero, C. Estarellas, A. Frontera, D. Quiñonero, *Theor. Chem. Acc.* **2010**, *126*, 1–14.
[58] a) S. R. Choudhury, P. Gamez, A. Robertazzi, C.-Y. Chen, H. M. Lee, S. Mukhopadhyay, *Cryst. Growth Des.* **2008**, *8*, 3773–3784; b) S. R. Choudhury, B. Dey, S. Das, P. Gamez, A. Robertazzi, C.-Y. Chen, H. M. Lee, S. Mukhopadhyay, *J. Phys. Chem. A* **2009**, *113*, 1623–1627.
[59] M. Salas, B. Gordillo, F. J. González, *Arkivoc* **2003**, *11*, 72–88.
[60] MIPp was computed using the MOPETE computer program: F. J. Luque, M. Orozco, Universitat de Barcelona, Barcelona, **1998**.
[61] M. J. Frisch, G. W. Trucks, H. B. Schlegel, G. E. Scuseria, M. A. Robb, J. R. Cheeseman, J. A. Montgomery Jr., T. Vreven, K. N. Kudin, J. C. Burant, J. M. Millam, S. S. Iyengar,

J. Tomasi, V. Barone, B. Mennucci, M. Cossi, G. Scalmani, N. Rega, G. A. Petersson, H. Nakatsuji, M. Hada, M. Ehara, K. Toyota, R. Fukuda, J. Hasegawa, M. Ishida, T. Nakajima, Y. Honda, O. Kitao, H. Nakai, M. Klene, X. Li, J. E. Knox, H. P. Hratchian, J. B. Cross, V. Bakken, C. Adamo, J. Jaramillo, R. Gomperts, R. E. Stratmann, O. Yazyev, A. J. Austin, R. Cammi, C. Pomelli, J. W. Ochterski, P. Y. Ayala, K. Morokuma, G. A. Voth, P. Salvador, J. J. Dannenberg, V. G. Zakrzewski, S. Dapprich, A. D. Daniels, M. C. Strain, O. Farkas, D. K. Malick, A. D. Rabuck, K. Raghavachari, J. B. Foresman, J. V. Ortiz, Q. Cui, A. G. Baboul, S. Clifford, J. Cioslowski, B. B. Stefanov, G. Liu, A. Liashenko, P. Piskorz, I. Komaromi, R. L. Martin, D. J. Fox, T. Keith, M. A. Al-Laham, C. Y. Peng, A. Nanayakkara, M. Challacombe, P. M. W. Gill, B. Johnson, W. Chen, M. W. Wong, C. Gonzalez, J. A. Pople, *Gaussian 03*, Revision C.02, Gaussian, Inc., Wallingford, CT, **2004**.

[62] N. Walker, D. Stuart, *Acta Crystallogr., Sect. A* **1983**, *39*, 158–166.

[63] L. J. Farrugia, *J. Appl. Crystallogr.* **1999**, *32*, 837–838.

[64] G. M. Sheldrick, *SHELXS86, Program for the Solution of Crystal Structures*, University of Göttingen, Göttingen, Germany, **1986**.

[65] G. M. Sheldrick, *Acta Crystallogr., Sect. A* **2008**, *64*, 112–122.

[66] G. M. Sheldrick, *SHELXL97, Program for Crystal Structure Analysis* (Release 97–2), University of Göttingen, Göttingen, Germany, **1997**.

Received: March 31, 2010
Published Online: July 13, 2010

